西北工業大學
NORTHWESTERN POLYTECHNICAL UNIVERSITY

SPHERIC

Progress of Smoothed Particle Hydrodynamics:

the Proceedings of the 2022 SPHERIC Xi'an International Workshop

Northwestern Polytechnical University
— Institute for Computational Mechanics and Its Applications

March 28th – April 2nd of 2022
Xi'an, Shaanxi, China

Acknowledgement

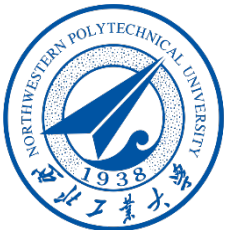

Northwestern Polytechnical University

(NPU)

Acta Mechanica Sinica

(AMS)

Joint International Research Laboratory of Impact Dynamics and its Engineering Application

Shaanxi Key Laboratory of Impact Dynamics and its Engineering Applications

Institute of Extreme Mechanics

(IEM)

Altair Engineering Inc.

(Nasdaq: ALTR)

About SPHERIC

Smoothed Particle Hydrodynamics rEsearch and engineeRing International Community (SPHERIC) is the international organization representing the community of researchers and industrial users of SPH.

As a purely Lagrangian technique, SPH enables the simulation of highly distorting fluids and solids. Fields including free-surface flows, solid mechanics, multi-phase, fluid-structure interaction and astrophysics where Eulerian methods can be difficult to apply represent ideal applications of this meshless method.

The SPH method was developed to study non-axisymmetric phenomena in astrophysics in the 1970s, but its application to engineering emerged in the 1990s and early 2000s. In the past twenty years the method has developed rapidly in many fields of application from impacts to fracture to breaking waves and fluid-structure interaction.

Following the impulse generated by a collection of local initiatives in 2005 (France, UK, Italy...), a need to foster and collaborate efforts and developments was identified. Since then, the SPHERIC organization has gone on to push the development of the method forward providing a network of researchers and industrial users around the world as a means to communicate and collaborate.

For more information about SPHERIC, please visit http://spheric-sph.org.

SPHERIC Xi'an 2022

It is a great honor to invite you to attend the 2022 SPHERIC Xi'an International Workshop (SPHERIC Xi'an 2022) to be held at Northwestern Polytechnical University in Xi'an, China, from March 28th to April 2nd of 2022. This is the third time that the workshop is held in China following the SPHERIC Beijing Workshop and SPHERIC Harbin Workshop.

The Workshop aims to share the latest theoretical developments and practical applications of the Smoothed Particle Hydrodynamics method. All articles on algorithm innovation and engineering applications of SPH method are welcomed.

On behalf of the organizing team, we are honored to warmly welcome scholars and students from all over the world to attend this workshop. Despite the impact of the epidemic, we can still meet each other online. Sincerely wish you a pleasant and satisfying experience in communication, training, and learning.

For more information about SPHERIC Xi'an 2022, please visit http://www.npuicma.cn/spheric2022.

About Northwestern Polytechnical University

Located in the historic city of Xi'an, the cradle of Chinese civilization and terminus of the ancient Silk Road, Northwestern Polytechnical University (NPU) is the only multidisciplinary and research-oriented university in China that is simultaneously developing education and research programs in the fields of aeronautics, astronautics, and marine technology engineering. It is now affiliated with the Ministry of Industry and Information Technology. Since the establishment of the Peoples Republic of China, NPU has always been one of the nation's key universities. It was one of the first universities to enter into the 211 Project in 1995 and the 985 Project in 2001. NPU is a member of the "Outstanding University Alliance" program and is honored as a National Role Model Unit, a National Pioneer for Optimal Advanced Basic-level Party Organization, and a Model University for Graduate Employment, etc. Over more than 80 years, NPU has built an outstanding academic reputation encapsulated in its motto of "Loyalty, Integrity, Courage, and Perseverance", and reflected in its spirit of "Strong Preparation, Diligent Effort, Practical Attitude, and Creative Innovation". As a key base for scientific research and innovation to cultivate high-level talents, NPU has been recognized as a "National Unit of Civilization" and awarded "the National Labor Medal". NPU was one of the first universities to establish a graduate school and national university science park, and now hosts the Northwest Institute of Industrial Technology and China's top UAV Research and Development Base. Now NPU will continue to pioneer new pathways into the future in the process of building a world first-class university and world first-class disciplines.

About School and Institute

School of Aeronautics, known as "the cradle of China's chief aircraft designers", has been devoted to training talents of aeronautics and implementing fundamental research since 1957. Institute for Computational Mechanics and Its Applications founded in 2012 is also a part of the School of Aeronautics. Aiming at the international frontier direction of computational mechanics and engineering applications, the institute is rooted in the profound background of computational mechanics, to develop new parallels meshless and particle methods, new efficient finite element methods, fast and high-precision of multiphase interface methods and other Frontier calculation methods and to integrate engineering simulation software with independent property rights. The institute is also committed to advanced technology research for engineering application by assisting the research and development of national engineering models and has successively undertaken tasks, such as ARJ21, C919 water runway taxiing simulation, AG600 water surface taxiing simulation, etc. During the 14th five-year plan period, the School of Aeronautics will follow the national strategic orientations, rely on its research platforms and international collaboration platforms, take opportunities of joint training projects of China Scholarship Council (CSC) and NPU, adjust international collaboration strategy, explore new ways to expand internationalized talent training and improve the quality of education for international students and the implement collaborative research.

Preface

The Institute for Computational Mechanics and Its Applications of Northwestern Polytechnical University is delighted to invite you to participate in the 2022 SPHERIC Xi'an International Workshop. This will be the premier event of 2022 in the field of Smoothed Particle Hydrodynamics (SPH) focusing on the method and applications.

The Smoothed Particle Hydrodynamics rEsearch and engineeRing International Community (SPHERIC) workshop is currently the only worldwide event exclusively focusing on presenting the latest theoretical developments and practical applications of SPH methodology. We have seen tremendous advances in the field of computational methods with this methodology. Thanks to the SPHERIC community for playing an important role in helping the development of SPH for academic, industry and government organizations. SPH in the field of computational methods will open up possibilities for research beyond any modeling capability, along with progress in specialized high-performance computing techniques.

2022 SPHERIC Xi'an International Workshop Organizing Committee has received more than 80 abstract submissions from China, Japan, Austria, Germany, Singapore, Spain, Italy, the United States, the United Kingdom, France, Ireland, and other countries, of which more than 50 have been selected for proceedings of SPHERIC Xi'an 2022. As a purely Lagrangian technique, SPH has been successfully applied in astrophysics, environmental engineering, ocean engineering, manufacture, geomechanics, biomechanics, and other fields, while related research covers free surface flow, solid mechanics, multi-phase, fluid-structure interaction, phase transition, etc. In the past two decades, SPH becomes one of the most efficient meshless particle methods in the fields of computational methods and has gained enhanced attention in the area of scientific computing.

It is a great pleasure to welcome you to SPHERIC Xi'an 2022, we are happy to meet you online and onsite. Let's treasure the chance to know each other in communicating.

Professor, Northwestern Polytechnical University

Chair, Local Organization Committee

SPHERIC Xi'an 2022

Table of Contents

Session 1: Fluid-structure Interaction I

Session 2: Solids and Fracture Mechanics I

Session 3: High-performance Computing

Session 4: Convergence, Consistency and Stability

Session 5: Applicability to Industry

Session 6: Thermal and Energy

Session 7: Fluid-structure Interaction II

Session 8: Viscosity and Turbulence

Session 9: Coupling to other Methods

Session 10: Multiple Continua and Multi-phase Flow

Session 11: Solids and Fracture Mechanics II

Session 12: Adaptivity and Variable Resolution

Session 13: Free Surfaces and Moving Boundaries

Session 14: Alternative and Novel Formulations

Three hours real–time SPH simulation of sloshing flows inside a LNG ship with realistic severe sea-state forcing

C. Pilloton, A. Colagrossi, S. Marrone
CNR-INM (Institue of Marine Engineering)
via di vallerano 139,
Rome, Italy
chiara.pilloton@inm.cnr.it

A. Bardazzi
University of Campania
"Luigi Vanvitelli"
Aversa, Italy
andrea.bardazzi@unicampania.it

***Abstract*—The present work is dedicated to the numerical investigation of three-dimensional sloshing flows inside a ship LNG fuel tank. Long time simulations, involving 3-hours real–time duration with realistic severe sea-state forcing, have been performed using a parallel SPH solver running for several weeks on a dedicated cluster. The adopted SPH method relies on a weakly-compressible approach and a Riemann Solver for the calculation of the particle interactions. The latter increases the stability of the scheme and allows for accurate predictions of the pressure during water impact stages (see also [26]). The intrinsic properties of mass and momenta conservation makes it well adapted for the simulation of such kind of violent free-surface flows for long-time evolution. Single phase model has been adopted with a considerable reduction of the CPU costs (for an in-depth discussion see also [27]). The high values of Reynolds numbers involved requires the implementation of a sub-scale model which was embedded in the SPH scheme following the recent literature (see *e.g.* [9]). Three different filling height conditions are considered. For all of them energetic sloshing flows are induced with the occurrence of several water impact events. The latter are focused on specific zones of the tank depending on the considered filling height (see also [15]). For some conditions the SPH pressure predictions are compared with the experimental ones provided by Hyundai Heavy Industries (HHI). A critical discussion of these predictions is performed in order to highlight in which cases the numerical solver is able to provide good local loads estimations. Conversely, when the SPH results appear to be not realistic, comments on the causes linked to the disagreements with experiments are given.**

I. Introduction

In the recent years, the consumption of the Liquefied Natural Gas (LNG) fuel has largely increased, caused by the commitment of nations to reduce noxious emissions of standard fuels. The storage and transportation of LNG have some specific issues that influence hardly carries design and their realization: the tank which has the task of keeping the liquid at a low temperature (-165 ^{o}C), called the Cargo Containment System (CCS), is a fundamental component. The CCS is built of a composite structure made by a metal membrane and a core of polyurethane foam and plywood in order to insulate the liquid. The structure is sized to resist the loads due to the liquid sloshing characterized by impulsive impacts induced by slamming motion. Its preservation is one of the main goal in the methodology of the design of new generation carries (for details see [16]). Despite the performance of materials and production processes are reaching ever higher levels of precision and quality, the LNG sloshing loads and impacts can damage the insulation tank under both high-fill and partial-fill conditions, as occurred in the past and reported in [14]. From the experimental point of view, small-scale tests have been evaluated due to the complexity of the sloshing flow features and its stochastic characteristic (see [10]; [19] and [20]; and [33]). These characteristics have also been an obstacle for numerical simulations. Nowadays, thanks to the increased computing power, sloshing simulations can be carried out for a long-time period of duration (beyond $1,000$ cycles) performing a statistical approach as required by modern industrial requests. The purpose of this paper is to present the results of the of long-time numerical sloshing simulations inside ship LNG tanks forcing by realistic severe sea-state, carried out with an enhanced Smoothed Particle Hydrodynamics (SPH) model. The tank model adopted is owned by Hyundai Heavy and the numerical results are compared with the experimental results achieved by Seoul National University (see [2] and [15]; [2] and [1]). It is important to underline some aspects related to this research:

- There are no publications, to the authors' knowledge, on simulating sloshing flows with such a long-time duration with the application of Navier-Stokes solvers.
- The CPU needed was very large: the maximum number of particles adopted is $400,000$ particles with about 10 millions time iterations. As a consequence, the temporal resolution, which depends on the spatial discretization, allowed a numerical time sampling rate of 9 kHz, which is of the same order of the experimental sampling rate of 20 kHz.
- Validations of numerical results required a statistical analysis and the data processing procedures of the SPH results have been compared consistently with the experimental time signals.

II. Description of the physical problem

The problem consists in a LNG tank, whose geometry is shown in figure 1 together with the pivot positions, subjected to a prescribed motion in all the 6 degrees of freedom (6-DOF) and it is partially filled with water. The total height of the tank is 20.77 m and three different filling height conditions are studied:

- 30% Small water filling height case, labelled as **SW** ,
- 60% Intermediate water filling height case, labelled as **IW** ,
- 90% Deep water filling height case, labelled as **DW** .

Each of these conditions were subjected with different 6-DOF time histories representing a realistic and severe sea conditions, taking as a reference the motions of a ship travelling in the North Atlantic route (significant wave height envelope fitted to 40 year return period). The time history of the dynamic is generated using a Pierson-Moskowitz spectrum with significant wave height 11.1 m and zero crossing period 9.5 sec in a heading angle condition of 90 °. The ship motions are evaluated through the spectrum with a 3D solver based on potential flow (see for more details [24]). The most excited degrees of freedom, under these sea conditions, are heave, sway and roll motions; in particular the heave motion presents a maximum amplitude of about 18 meters, the horizontal oscillations vary in the range between $[-5, +5]$ meters and the roll motion oscillates in the interval $[-2, +2]$ degrees. The SPH simulations are performed at the same scale used in the experiment model that is $\lambda = 1 : 50$. In sloshing problem the main flow features are mostly driven by the Froude number and the quantities of SPH results are scaled to the real size by respecting the Froude scaling (when not otherwise specified).

Given the tank dynamic involved, the Reynolds number is very high, $O(10^6)$ and a very high resolution should be needed to resolve the boundary layer. However, since the boundary layer is expected to play a minor role, a Large Eddy Simulations model is implemented and the sub-grid vortical structures are modelled with a classical Smagorinsky law.

LNG fuel tank dimension for One-row tank

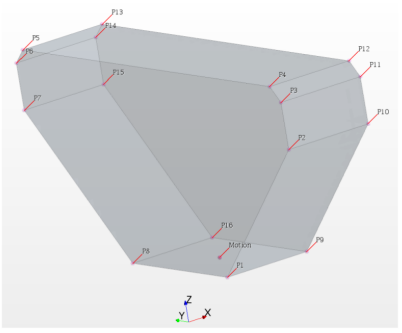

	X [m]	Y [m]	Z [m]
P1	0	-8.031	5.305
P2	0	-22.44	19.714
P3	0	-22.44	24.556
P4	0	-20.951	26.045
P5	0	20.951	26.045
P6	0	22.44	24.556
P7	0	22.44	19.714
P8	0	8.031	5.305
P9	9.86	-8.031	5.305
P10	9.86	-22.44	19.714
P11	9.86	-22.44	24.556
P12	9.86	-20.951	26.045
P13	9.86	20.951	26.045
P14	9.86	22.44	24.556
P15	9.86	22.44	19.714
P16	9.86	8.031	5.305

	X [m]	Y [m]	Z [m]
Motion	4.93	0	5.305

Fig. 1. LNG tank geometry in real scale with the coordinates of the different vertices and the position of the Pivot for the constrained motion.

Arrangement of pressure sensors

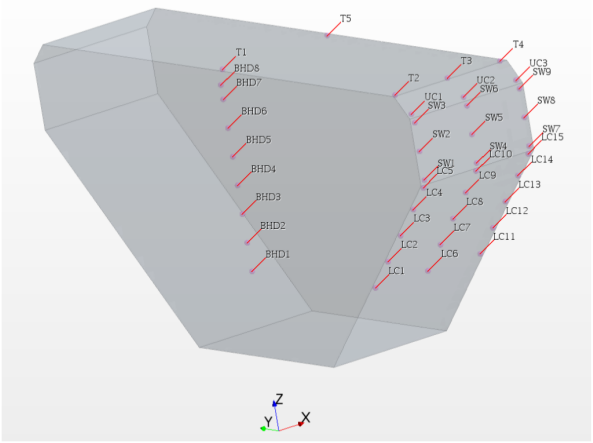

Fig. 2. Sketches of the tank geometry with labels and positions of the different pressure probes.

This strategy allows the use of a uniform spatial resolution in simulation and thus, a free-slip condition at the tank walls. Figure 2 reports the labels and positions of the different pressure probes used in the experiments as well as in the SPH simulations. For all the three test conditions some flow features related to critical impact events have been considered in section V.

Before running the 3D long-time simulations, in the first phase of the study, a 2D preliminary tests were carried out on the three filling-heights in order to verify the parameter choice, the tank motion, the CPU costs and to define the size of the particles and if the time step is small enough to guarantee a good pressure evaluation during impact events.

III. Governing equations

The governing equations adopted in this work are the Navier-Stokes equations (NSE) for a single-phase weakly compressible fluid. Since the Reynolds number of the flow is quite high, a sub-scale grid model has been adopted. The equations solved, written in a Lagrangian formalism are:

$$\begin{cases} \dfrac{D\rho}{Dt} &= -\rho\,\nabla\cdot\mathbf{u} \\ \rho\dfrac{D\mathbf{u}}{Dt} &= -\nabla p + \rho\,\mathbf{g} + (\mu+\mu_T)\nabla^2\mathbf{u} \\ \dfrac{D\mathbf{r}}{Dt} &= \mathbf{u}\,, \qquad p = c_0^2(\rho-\rho_0) \end{cases} \tag{1}$$

where D/Dt represents the Lagrangian derivative, while $\mathbf{r}$, $\mathbf{u}$, p and ρ are, respectively, the position of a generic material point, its velocity, pressure and density while $\mathbf{g}$ represents gravitational acceleration. Regarding the viscous term in the momentum equation μ is the fluid viscosity while μ_T indicates the local turbulent viscosity.

The fluid is assumed to be barotropic and a simple linear equation of state is used, where ρ_0 is the density of the liquid at the free surface and c_0 is the artificial speed of sound. The weakly-compressible regime implies the following requirement:

$$c_0 \geq \max\left(10U_{max}, 10\sqrt{\frac{(\Delta p)_{max}}{\rho}}\right) \quad (2)$$

where U_{max} and $(\Delta p)_{max}$ respectively are the maximum fluid speed and the maximum pressure variation expected (with respect to the zero pressure free-surface level) in the fluid domain (see [27]). Constraint (2) however, has to be respected to guarantee the weakly-compressible regime and this condition has to be verified throughout the simulations.

For the present study, the proper identification of c_0 is crucial, as it will be discussed in the following sections. Constraint (2) ensure that compressibility effects are negligible (i.e. density variations smaller than 1%). However, during violent impact events (i.e., flat impacts) the acoustic pressure $p = \rho\, u\, c_0$ can be reached, and in this case the pressure peak intensity becomes proportional to 1/Ma. On the other hand, in such a condition an incompressible constraint can induce singularities on the pressure field. This is linked to the fact that for this kind of impacts the presence of the air phase is generally crucial and the single-phase approach can lead to incorrect pressure evaluations under the incompressible/weakly-compressible hypothesis.

Being aware of these limits for a single-phase model, the results obtained in this work have been critically revised considering a possible Mach dependency. For a more in-depth discussion on this topic see also [25], [27], [28].

IV. Numerical Model

Violent sloshing flows can be simulated using different numerical methods. In the recent years Finite Volume Methods coupled with Volume-of-Fluids algorithm have been extensively used for simulating such kind of flows (see for example [11], [12], [17], [18], [22], [23]). Beside mesh-based solver also Particle Methods like the Smoothed Particle Hydrodynamics (SPH) models have been proved to be powerful numerical solvers for tackling violent sloshing flows. Regarding SPH simulations of sloshing flows, during recent years a thorough validation has been carried out (see *e.g.* [3]–[6], [8], [13], [32])

In the present work a Riemann-based variant of the classical SPH scheme is adopted. This specific scheme has been adopted for the following reasons:

- the high accuracy in the prediction of pressure liquid impacts (see *e.g.* [25], [26]);
- the high robustness of the scheme which helps handling long-time simulations;
- the good volume conservation properties when simulating long-time violent free-surface flows, while for other SPH schemes, like the popular δ^+-SPH schemes, special treatments are needed as discussed recently in [21];
- the treatment of wall boundary condition: within the Riemann-SPH model the new developments described in [7] were implemented. The latter is based on a boundary integral approach based on a cutface process for calculating the particle–wall interactions on geometries of arbitrary shapes.

In the specific, the adopted Riemann-SPH scheme is the one proposed by [29], characterized by zero mass fluxes. A MUSCL (Monotone Upstream Scheme for Conservation Laws) procedure is used to increase the order of this Total Variation Diminishing (TVD) scheme. Thanks to the introduction of Riemann-solvers the fluxes between particles are upwind oriented and the resulting scheme is more stable. The viscous term adopted contains both the effect of the fluid viscosity μ as well as the one related to the local turbulent viscosity (for details see [9]).

A. The adopted Software and Hardware

In order to perform the three long-time 3D simulations for the cases **SW**, **IW** and **DW** some ad-hoc computing blades have been used. The characteristic of the three blades are:

- BLADE N° 1: 64 cores AMD Opteron (tm) Processor 6376, 2.30GHz
- BLADE N° 2: 64 cores Intel(R) Xeon(R) CPU E5-2698 v3, 2.30GHz
- BLADE N° 3: 64 cores Intel(R) Xeon(R) CPU E5-2698 v3, 2.30GHz

Since the blade N° 1 has lower CPU performance, it is dedicated to the **SW** case; this case indeed involves a lower number of particles with respect to the other two cases, **IW** and **DW**, as explained in the next section IV-B. The blade N° 1 has been also used to perform the preliminary 2D analysis.

As a software the SPH-flow code was used, indeed, starting from 2013 CNR-INM participated in building a consortium with the Ecole Centrale de Nantes (ECN) and a Company called NextFlow-Software for developing this industrial SPH code.

The SPH-flow solver has been tested on those new blades by evaluating the CPU costs per iteration and per particle for a single computing core in order to get a prediction of the maximum time and spatial resolutions to be adopted for the three simulations. The results of these preliminary tests on the software performance is reported in table I; those results are used in the next sections to fix the parameters for the 3D simulations. The last column of table I shows the CPU-efficiency defined as the time needed to the SPH-flow software to perform one iteration divided by the number of particles presented in the domain and multiplied by the number of cores used. This number allows to get a prediction of the CPU costs and, therefore, to set the maximum number of particles and the maximum number of time iterations for the given computational resources. The CPU-efficiency depends:

- on the ratio $h/\Delta r$ or, in other words, on the number of particle neighbors;
- on the characteristics of the specific CPU adopted;

- on the peculiarities of the simulation which may influence the parallelization efficiency (e.g. presence of boundaries, extension of the domain).

Blade N°	N° of cores	$N_{particles}$	$h/\Delta r$	CPU-efficiency (seconds $\times 10^{-6}$)
1	60	370,000	1.05	260
2	60	400,000	1.05	124
3	60	480,000	1.1	156

TABLE I
EVALUATION OF THE CPU-FACTOR. THE CPU-FACTOR IS THE TIME NEEDED TO THE SPH-FLOW SOFTWARE TO PERFORM ONE ITERATION DIVIDED BY THE NUMBER OF PARTICLES PRESENTED IN THE DOMAIN AND MULTIPLIED BY THE NUMBER OF CORES USED.

B. Set-up of the simulation parameters

In order to set-up the parameters for the 3D simulations we need to specify the time and the space discretizations for the available CPU resources. The SPH equations are integrated in time by using a fourth-order Runge-Kutta scheme. The time step is obtained as:

$$\Delta t \leq CFL \left(\frac{\Delta r}{c_0}\right)\left(\frac{h}{\Delta r}\right),$$

where the Courant-Friedrichs-Lewy constant is $CFL = 0.6$ for a Wendland C2 Kernel. To ensure the weakly-compressibility, the sound speed has been chosen to satisfy the requirement (2).

For the case **SW** the maximum velocity field expected in the tank can be estimated as $U_{max} = \sqrt{gH}$ being H the filling height, and the speed of sound is therefore set as $c_0 \geq 10\sqrt{gH}$. For the case **DW** the p_{max} pressure can be estimated with the maximum hydrostatic pressure $p_{max} = \rho g H$, and therefore the speed of sound is again $c_0 \geq 10\sqrt{gH}$. The above estimation implies that for the **DW** case a larger speed of sound is needed, $c_0 = 140$ m/s. Furthermore, the **DW** case has a larger fluid domain to be discretized. This means that we cannot use the same spatial discretization for the **SW** and the **DW** cases, if we want to use the computing blades in an efficient way. Even if the speeds of sound for the cases **SW** and **IW** can be set in principle equal to, respectively, $c_0 = 80$ and 110 m/s, we prefer to use higher values, specifically $c_0 = 120$ and 140 m/s, since we expect for these cases slamming loads of the same order of magnitude as in the case **DW** . Using the above information and the CPU-efficiency evaluated in the previous section, the parameters for the 3D simulations can be set and the total CPU costs can be estimated.

C. Effects and limits of the SPH compressibility during violent impacts

Since in this research investigation the sloshing simulations are characterized by large motions and violent impact events, the estimation on the maximum velocity and pressure values, used in the previous section to set c_0, can be locally overpassed. For this reason a preliminary 2D simulation was conducted to evaluate the maximum velocity of the fluid during the impact stages. For the **SW** case we found that the fluid velocity just before the impact is about 15 m/s which is just 16% greater than the one predicted in the previous section. It is important to note that the fluid velocity can be even higher than 15 m/s but only for very local fluid portions, like single drops generated by the fragmentation of water jets.

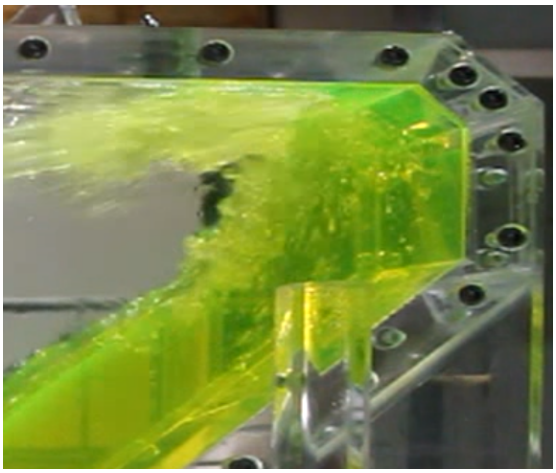

Fig. 3. **SW** case. Enlarged view of a picture taken from the experiment during an impact event. The presence of air bubbles inside the bulk of the fluid is evident.

A correct setting of the magnitude of the fluid velocity is necessary but not sufficient to ensure that compressible effects are negligible. Indeed, also the pressure has to be taken into account. During impact stages, depending on the water jet geometry, the water-hammer pressure can be reached because of the absence of the air phase. This pressure is equal to $\rho\, c_0\, U_{jet}$ and, therefore, it is strongly dependent on the choice made on the speed of sound. Using c_0 in the range 120 - 140 m/s leads to water-hammer pressure of about 20 bar (in real scale, which correspond to 40 kPa in model scale). When the water-hammer pressures are reached the weakly-compressible limits are exceeded and the compressibility starts to play a too relevant role indicating that a two-phase model is needed for a better prediction. It is important to note that the adoption of c_0 in the range 120–140 m/s corresponds to the speed of sound of fresh water with 1% of air dispersed as bubbles (for more details see [30]). From figure 3 it is possible to see that different air-bubbles are present in the bulk of the fluid during violent impacts. In this way in our SPH model we estimate 1% of air entrapped in the water. However, the model adopted cannot take into account the bubble spatial distribution nor the sizes of the entrapped bubbles. The air bubbles largely influence the rise time and the time duration of the pressure peaks and, thus, we do not expect that SPH will be able to accurately predict those quantities.

On the other hand, it is worth noting that when in our model the pressure hammer limit is reached it means that using an incompressible solver the pressure peak would be unbounded and proportional to $1/\Delta t$. Therefore, with an incompressible solver the pressure peak in those cases are completely depen-

dent on the time-space resolution adopted in the simulations. This is not the case for the SPH simulations thanks to the limit linked to c_0 which, in any case, is strictly dependent on the estimation of the volume fraction of air in water during the impact event.

D. Preliminary 2D simulations with different spatial resolutions

In order to verify that the spatial resolutions, identified in the previous section, are fine enough to get pressure evaluations which are weakly dependent on the particle size, some tests in the 2D framework have been performed. The case **SW** has been selected for this preliminary analysis and different pressure probes are considered in order to check the effect of the Δr parameter.

Three different spatial resolutions $H/\Delta r = 20, 40, 80$ are used in order to check the dependency of the pressure peaks recorded by this parameter. The conclusions of the 2D analysis are that the resolutions $H/\Delta r = 40, 60$ and 80 can be a good compromise, in terms of accuracy and computational costs, for conducting 3D simulations of the **SW** , **IW** and **DW** cases, respectively. The interested reader can find more details in [31].

V. Discussion of the results

In this section the analysis of the pressure time histories calculated with the SPH 3D simulations is performed for the three different cases: **SW** , **IW** and **DW** . The most critical probes are here examined and discussed. Specifically, for each filling height we selected the most critical probes, analyzing in detail the pressure time history. The selected probes are:

- SW7 probe for the **SW** case
- UC3 probe for the **IW** case
- T4 probe for the **DW** case:

Each filling condition is treated in separate subsections.

A. SW case

The **SW** case is characterized by very large water displacements and deformations. Figure 4 depicts the particle configuration during an impact event: when the pressure at the wall reaches its maximum. Because of the violent impact the water jet hitting the tank roof is fragmented in several drops. This flow condition can be critical for mesh-based solver since the size of those drops can be of the order of the mesh-size and, therefore, some of them can be numerically canceled, resulting in a progressive reduction of the water mass. Those kinds of error can be quite critical in long-time simulations where several water impacts take place. Conversely, thanks to the intrinsic mass conservation of the SPH scheme the small drops consisting in single SPH particles are always tracked until they get back into the bulk of the fluid. Figure 5 shows for the probe SW7 the plot of the pressure peaks versus their rise time. The quantities in these plots have been reported in model scale to simplify the comparison with the experimental data. For the probe SW7 the number of the impact events registered is

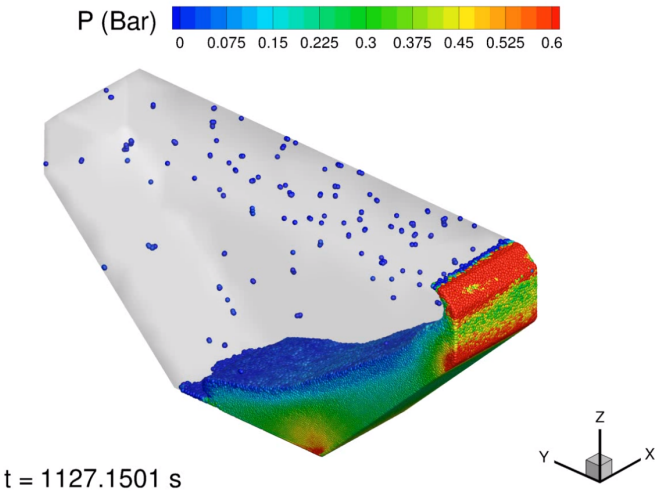

Fig. 4. Case **SW** : particles configuration during an impact event. Colors are representative of the pressure field in real scale.

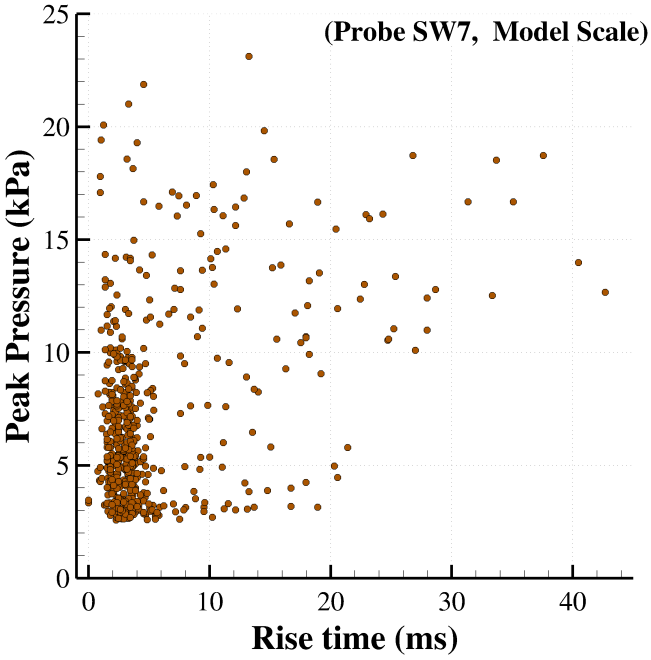

Fig. 5. Case **SW** : SPH pressure peak vs rise time for probe SW7 (quantities are reported in model scale).

very high, 573. As we already commented in section IV-C this pressure regime is related to the hammer pressure level. The maximum experimental pressure peak recorded is about 30 kPa whereas the maximum SPH pressure recorded is about 23 kPa. The magnitude of the recorded SPH pressure is comparable with the experimental data but this is not the case for the rise time. The SPH predicts a rise time of about 15 ms while in the experiments it is about 2.3 ms. The main reason of this discrepancies is probably linked to:

- the low sampling rate of the SPH simulation, 9 kHz, with respect to the 20kHz adopted in the experiments. The SPH

sampling rate is linked to the spatial resolution adopted in the simulations, therefore the use of higher resolution can improve the evaluation of the rise time.
- the use of a single-phase model; in reality the time duration of the pressure peaks are, indeed, mainly linked to the air pockets entrapped in the water which induce shorter time rises.
- because of the interpolation through kernel function SPH tends to predict a pre-loading before the actual pressure peak; this aspect contribute to the increase of the computed time rise.

More research is needed on this topic also to determine the effect of the weakly-compressible model adopted on this specific aspect and to develop possible solutions in order to improve the solvers prediction.

B. IW case

The SPH prediction for the case with intermediate filling height, H=12.44 m, is discussed in this section. This case can be the most critical in some conditions, indeed the filling height still allows large motions of the sloshing flow and, at the same time, it is high enough for the liquid to reach and violently impact the tank roof. Figure 6 shows the particle configuration during an impact event. The number of impacts on the probes T2 and T4 is about 350 while for the **SW** case is about 250. Probes SW1 and SW7 are the ones where the largest number of impacts is recorded: about 500 events.

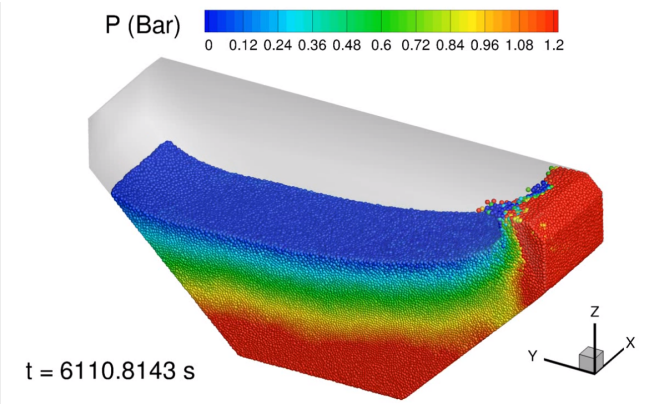

Fig. 6. Case **IW** : particles configuration during an impact event. Colors are representative of the pressure field in real scale.

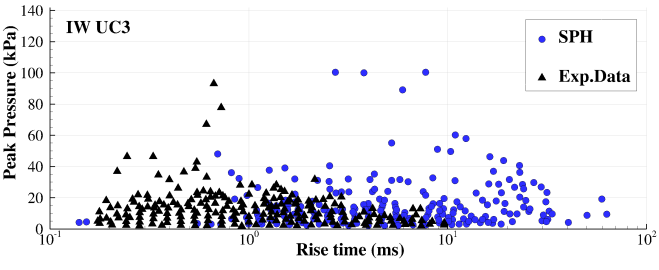

Fig. 7. Case **IW** . Comparison SPH vs experiments of scatter diagram for peak pressure and rise time at 60%H filling for the probe UC3. The data are reported for the model scale.

Figure 7 depicts the comparisons between SPH and experiments within a scatter diagram where peak pressure and rise time for the **IW** case are plotted for probe UC3. From this diagram the same conclusions of the **SW** case can be drawn: the SPH is able to well predict the pressure peak ranges while the rise times are generally overestimated. From the figure it is possible to see that critical events with pressure intensity above 100 kPa (50 bar at real scale) are registered. The same pressure level is also reached in the experiments but just for a single impact event. This pressure level is above the limit of the hammer pressure defined in section IV-C or, in other words, this impact is largely affected by the selected speed of sound c_0 (see sections III and IV-C). With a c_0 equal to 20 m/s (model scale), the pressure level of 100 kPa implies a compressibility of the water-air mixture of $\Delta\rho/\rho$ of about 25%. This means that for these critical events the adopted model is being strained beyond its limits of applicability. It is worth noting that the extreme events $P > 100$ kPa were not predicted by the 2D preliminary analysis this means those events are related to peculiar 3D flow features. The latter are linked to void cavities formed close to the roof vertex which quickly shrinks due to the approaching jets. In the reality this cavity would be filled with air and would induce an oscillating pressure on the probes according to the characteristic air bubble vibration period. Conversely, in the present calculation the void pocket collapses giving rise to a violent fluid-fluid impact which reaches the water hammer pressure limit. This justify why in the SPH simulation the extreme events $P > 100$ kPa happen more frequently than in the experiments.

C. DW case

Finally, in the present subsection the case **DW** , which is characterized by the highest filling height $H = 18.67$ m, is discussed. Figure 8 shows a particle configuration during a roof impact event. This case is characterized by numerous roof impacts and the most critical pressure probes are T2, T3, T4, most of the other probes being completely immersed. The SW3, SW6, SW9 are just 55 cm above the still water level

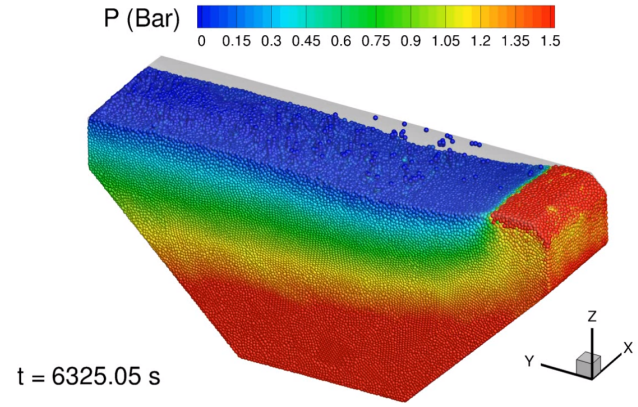

Fig. 8. Case **DW** : SPH 3D simulation, particles configuration during an impact event. Colors are representative of the pressure field at real scale.

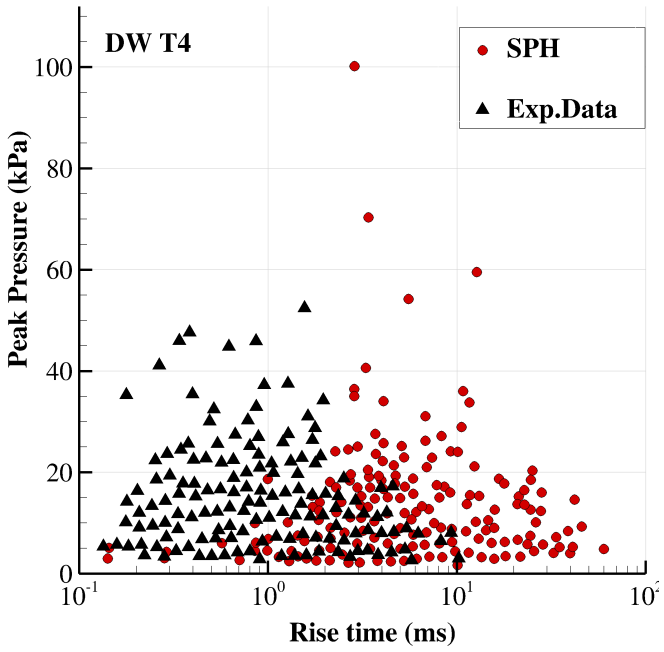

Fig. 9. Case **DW** . Comparison of scatter diagram for peak pressure and rise time at 90%H filling for the probe T4. The data are reported for the model scale.

while the UC probes are at a distance of 88 cm. Because of the above observations, in the following analysis only the probes T2, T3, T4 and UC3 are considered; indeed, for each of these, more than 1100 impact events are recorded. Beside this, we note that critical impact events are also recorded at probes SW1 and SW7.

Figure 9 shows the scatter diagrams of peak pressure and rise time for the **DW** case for the probe T4. A part two extreme events recorded by the SPH, also for the highest filling height condition the SPH is able to predict the pressure peak ranges in a fair accordance with the experiments while the rise times are again overestimated; the SPH range is between 1 to 90 milliseconds, much larger than the one experimentally measured.

For the probes of the group T, similarly to what shown in the previous case for other tank positions, some violent events induce pressure levels higher than 50 kPa in model scale, which is quite close to the pressure hammer estimated by the 2D preliminary analysis using the maximum of the velocity field (see section IV-C).

Figure 10 reports an experimental picture taken during the **DW** case (but in a different reference sea-state condition). The middle and the bottom plots of the same figure depicts the time histories for two pressure peak measured in the proximity of the T-group probes. It is interesting to note that the peak pressure intensities are around 80 kPa, hence, quite close to the most energetic events evaluated by the SPH model.

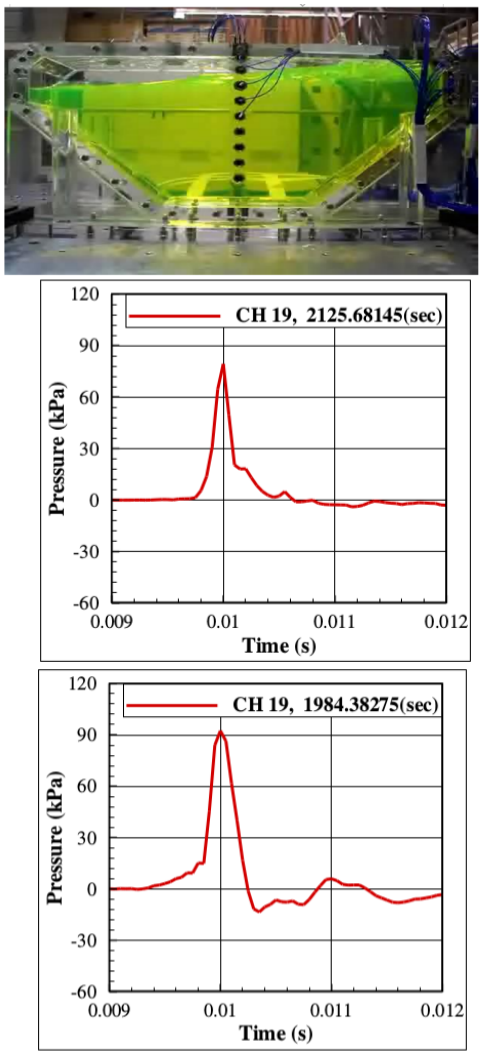

Fig. 10. Case **DW** : Top: picture taken during experiments performed with a sea-state given by a Pierson-Moskowitz spectrum with significant wave height 8.3 m and zero crossing period 7.50 sec with an angle condition of 120°. Middle and bottom: time history of pressure peaks measured at the probe T4 position (quantities are reported in model scale).

VI. Conclusions

In the present work the numerical investigation of sloshing flows inside a ship LNG fuel tank was studied. Long time simulations, involving 3-hours real–time duration with realistic severe sea-state forcing, were performed using the parallel CFD software called SPH-Flow which ran for several weeks on a dedicated cluster. 3D simulations with 3 different water depths have been launched. They have run for about six months on three dedicated blades, each of those equipped with 64 cores. After that a post-processing stage has been conducted in order to analyze the pressure time histories on 40 different probes. For the most critical events an analysis of the flow features has been also performed in order to better understand the obtained outcomes. The low filling case resulted to be by far the less critical condition. In the intermediate condition a

slightly larger number of extreme events have been registered with respect to the deep filling condition. The comparisons of the SPH outcomes with the experimental data shows that adopted SPH model is able to well predict the intensity of the pressure peaks while the numerical rise times are always overestimated.

Acknowledgment

The research activity was supported by the project SinSEOn "Sloshing SPH Environment for long-time Oscillation simulation", within the Memorandum of Understanding 2015-2018 between CNR-INM (formerly CNR-INSEAN) and the Hyundai Maritime Research Institute (HMRI) of Hyundai Heavy Industries Co. Ltd. The work was partially supported by the SLOWD project which received funding from the European Union's Horizon 2020 research and innovation programme under grant agreement No 815044. The SPH simulations performed under the present research were obtained using the SPH-Flow solver, software developed within a collaborative consortium composed of Ecole Centrale Nantes, NextFlow Software company and CNR-INM.

References

[1] Yangjun Ahn and Yonghwan Kim. Data mining in sloshing experiment database and application of neural network for extreme load prediction. *Marine Structures*, 80:103074, 2021.

[2] Yangjun Ahn, Yonghwan Kim, and Sang-Yeob Kim. Database of model-scale sloshing experiment for lng tank and application of artificial neural network for sloshing load prediction. *Marine Structures*, 66:66–82, 2019.

[3] Benjamin Bouscasse, Matteo Antuono, Andrea Colagrossi, and Claudio Lugni. Numerical and experimental investigation of nonlinear shallow water sloshing. *International Journal of Nonlinear Sciences and Numerical Simulation*, 14(2):123–138, 2013.

[4] Benjamin Bouscasse, Andrea Colagrossi, Antonio Souto-Iglesias, and JL Cercos-Pita. Mechanical energy dissipation induced by sloshing and wave breaking in a fully coupled angular motion system. I. theoretical formulation and numerical investigation. *Physics of Fluids*, 26(3):033103, 2014.

[5] Benjamin Bouscasse, Andrea Colagrossi, Antonio Souto-Iglesias, and JL Cercos-Pita. Mechanical energy dissipation induced by sloshing and wave breaking in a fully coupled angular motion system. II. experimental investigation. *Physics of Fluids*, 26(3):033104, 2014.

[6] XY Cao, FR Ming, and AM Zhang. Sloshing in a rectangular tank based on SPH simulation. *Applied Ocean Research*, 47:241–254, 2014.

[7] L. Chiron, M. De Leffe, G. Oger, and D. Le Touzé. Fast and accurate SPH modelling of 3d complex wall boundaries in viscous and non viscous flows. *Computer Physics Communications*, 234:93–111, 2019.

[8] L Delorme, A Colagrossi, A Souto-Iglesias, R Zamora-Rodriguez, and E Botia-Vera. A set of canonical problems in sloshing, part i: Pressure field in forced roll—comparison between experimental results and SPH. *Ocean Engineering*, 36(2):168–178, 2009.

[9] A. Di Mascio, M. Antuono, A. Colagrossi, and S. Marrone. Smoothed particle hydrodynamics method from a large eddy simulation perspective. *Physics of Fluids*, 29(3):035102, 2017.

[10] Louis Diebold and Eric Baudin. Bureau veritas sloshing model tests & CFD calculations for isope sloshing benchmark. In *The Twenty-fourth International Ocean and Polar Engineering Conference*. OnePetro, 2014.

[11] R. Elahi, M. Passandideh-Fard, and A. Javanshir. Simulation of liquid sloshing in 2d containers using the volume of fluid method. *Ocean Engineering*, 96:226–244, 2015.

[12] Je. Gómez-Goñi, C.A. Garrido-Mendoza, J.L. Cercós, and L. González. Two phase analysis of sloshing in a rectangular container with volume of fluid (vof) methods. *Ocean Engineering*, 73:208–212, 2013.

[13] Mashy D Green and Joaquim Peiró. Long duration SPH simulations of sloshing in tanks with a low fill ratio and high stretching. *Computers & fluids*, 174:179–199, 2018.

[14] Pierre Jean and Henri Petit. Methane by sea—a history of french methane carrier techniques. *France: Gaz Transport & Technigaz*, 1998.

[15] Sang-Yeob Kim, Yonghwan Kim, and Jaehoon Lee. Comparison of sloshing-induced pressure in different scale tanks. *Ships and Offshore Structures*, 12(2):244–261, 2017.

[16] JF Kuo, RB Campbell, Z Ding, SM Hoie, AJ Rinehart, RE Sandström, TW Yung, MN Greer, and MA Danaczko. LNG tank sloshing assessment methodology-the new generation. In *The Nineteenth International Offshore and Polar Engineering Conference*. OnePetro, 2009.

[17] D.H. Lee, M.H. Kim, S.H. Kwon, J.W. Kim, and Y.B. Lee. A parametric sensitivity study on lng tank sloshing loads by numerical simulations. *Ocean Engineering*, 34(1):3–9, 2007.

[18] H.T. Li, J. Li, Z. Zong, and Z. Chen. Numerical studies on sloshing in rectangular tanks using a tree-based adaptive solver and experimental validation. *Ocean engineering*, 82:20–31, 2014.

[19] Thibaut Loysel, Sabrina Chollet, Eric Gervaise, Laurent Brosset, and Pierre-Emmanuel De Seze. Results of the first sloshing model test benchmark. In *The Twenty-second International Offshore and Polar Engineering Conference*. OnePetro, 2012.

[20] Thibaut Loysel, Eric Gervaise, Sylvestre Moreau, and Laurent Brosset. Results of the 2012-2013 sloshing model test benchmark. In *The Twenty-third International Offshore and Polar Engineering Conference*. OnePetro, 2013.

[21] H.G. Lyu and P.N. Sun. Further enhancement of the particle shifting technique: Towards better volume conservation and particle distribution in SPH simulations of violent free-surface flows. *Applied Mathematical Modelling*, 101:214–238, 2022.

[22] W. Lyu, O. el Moctar, R. Potthoff, and J. Neugebauer. Experimental and numerical investigation of sloshing using different free surface capturing methods. *Applied Ocean Research*, 68:307–324, 2017.

[23] A.G. Malan, B.W. Jones, L.C. Malan, and M. Wright. Accurate prediction of violent slosh loads via a weakly compressible vof formulation. In *The 31st International Ocean and Polar Engineering Conference*. OnePetro, 2021.

[24] S. Malenica, F.X. Sireta, F. Bigot, C. Wang, and X.B. Chen. Some aspects of hydro-structure coupling for combined action of seakeeping and sloshing. In *International Conference on Offshore Mechanics and Arctic Engineering*, volume Volume 6: Materials Technology; C.C. Mei Symposium on Wave Mechanics and Hydrodynamics; Offshore Measurement and Data Interpretation, pages 461–467, 05 2009.

[25] S. Marrone, A. Colagrossi, A. Di Mascio, and D. Le Touzé. Prediction of energy losses in water impacts using incompressible and weakly compressible models. *Journal of Fluids and Structures*, 54:802–822, 2015.

[26] S Marrone, A Colagrossi, JS Park, and EF Campana. Challenges on the numerical prediction of slamming loads on lng tank insulation panels. *Ocean Engineering*, 141:512–530, 2017.

[27] Salvatore Marrone, Andrea Colagrossi, Andrea Di Mascio, and David Le Touzé. Analysis of free-surface flows through energy considerations: Single-phase versus two-phase modeling. *Physical Review E*, 93(5):053113, 2016.

[28] DD Meringolo, A Colagrossi, S Marrone, and F Aristodemo. On the filtering of acoustic components in weakly-compressible SPH simulations. *Journal of Fluids and Structures*, 70:1–23, 2017.

[29] Anatoly N Parshikov and Stanislav A Medin. Smoothed particle hydrodynamics using interparticle contact algorithms. *Journal of computational physics*, 180(1):358–382, 2002.

[30] DH Peregrine. Water-wave impact on walls. *Annual Review of Fluid Mechanics*, 35(1):23–43, 2003.

[31] C. Pilloton, A. Bardazzi, A. Colagrossi, and S. Marrone. SPH method for long-time simulations of sloshing flows in LNG tanks. *European Journal of Mechanics - B/Fluids*, 93:65–92, 2022.

[32] JR Shao, HQ Li, GR Liu, and MB Liu. An improved sph method for modeling liquid sloshing dynamics. *Computers & Structures*, 100:18–26, 2012.

[33] Zhijun Wei, Shilun Ruan, Xiaodong Chen, Song Luo, and Qianjin Yue. An experimental investigation of liquid sloshing impact load in a large-scaled prismatic tank. In *The Twenty-fourth International Ocean and Polar Engineering Conference*. OnePetro, 2014.